*International Journal on Recent and Innovation Trends in Computing and Communication*
*ISSN: 2321-8169 Volume: 11 Issue: 3s*
*DOI: https://doi.org/10.17762/ijritcc.v11i3s.6155*
***Article Received**: 01 December 2022 **Revised**: 04 January 2023 **Accepted**: 12 January 2023*

# Three Step Authentication of Brain Tumour Segmentation Using Hybrid Active Contour Model and Discrete Wavelet Transform

**Jayaraj Ramasamy[1], Dr. Ruchi Doshi[2], Dr. Kamal Kant Hiran[3]**
[1]Department of CSE
Azteca University
Chalco, Mexico
jayarajrcse@gmail.com
[2]Department of CSE
Azteca University
Chalco, Mexico
ruchi.doshi@univ-azteca.edu.mx
[3]Department of Computer Science and IT
Symbiosis University of Applied Sciences
Indore, India
kamalkant.hiran@suas.ac.in

**Abstract: -**
An innovative imaging research is expected in the medical field due to the challenges and inaccuracies in diagnosing the life-threatened harmful tumours. Brain tumor diagnosis is one of the most difficult areas of study in diagnostic imaging, with the maximum fine for a small glitch given the patients survival rate. Conventionally, biopsy method is used to identify the tumour tissues from the brain's soft tissues by the medical researchers (or) practitioners and it is unproductive due to: (i) it requires more time, and (ii) it may have errors. This paper presents the three-stage authentication-based hybrid brain tumour segmentation process and it makes the detection more accrual. Primarily, tumour area is segmented from a magnetic resonance image and after that when comparing a differentiated segment of an image to the actual image, an improved active contour model is employed to achieve a good match. In addition, discrete wavelet transform is used for the features extraction which leads to improve the accuracy and robustness in the tumour diagnosis. Finally, RELM classifier is used for precise classification of brain tumours. The most effective section of our method is checking the status of the tumour through finding the tumour region. The results are evaluated through new dataset, and it demonstrates that the suggested approach is more efficient than the alternatives as well as provides 96.25% accuracy.

## I. Introduction

A World Health Organization (WHO) report claims that estimate from preadolescence to adulthood, there were over 0.3 million cases of brain tumors reported in the year 2018 [1]. Brain tumours may generally be classified as malignant (having cancerous side effects) or benign (not having cancerous side effects), with each type being characterised by specific traits such tumour advancement rate and pattern [2].

Biopsy seems to be the current clinically accepted method for determining a brain tumour's diagnosis and selecting its course of treatment [3]. An intrusive operation like a biopsy has risks including hematoma [4]. Therefore, a non-invasive radiological biomarker based on neuroimaging that can distinguish between LGG and HGG cancers can significantly cut down on the expense, time, and possible consequences of surgery. Segmenting the parts of the brain tumour and the neighbouring healthy cells is necessary as the initial step in discovering neuroimaging-based biomarkers. Delineating the various tumour components, such as the necrotic zone, the active region, and the edoema around the tumour, is crucial in addition to tumour segmentation. It offers vital details regarding how a disease develops, how to design a course of treatment, and how well a patient responds to a certain therapeutic paradigm [5].

An expert radiologist frequently segments brain tumours manually using radiographic pictures. An automated repeatable segmentation technique or algorithm is needed because this is labour-intensive, subject to operator bias, and has low repeatability [6]. However, despite the ongoing,

*International Journal on Recent and Innovation Trends in Computing and Communication*
*ISSN: 2321-8169 Volume: 11 Issue: 3s*
*DOI: https://doi.org/10.17762/ijritcc.v11i3s.6155*
***Article Received**: 01 December 2022 **Revised**: 04 January 2023 **Accepted**: 12 January 2023*

rigors study in this area for more than 20 years, automated tumour segmentation still remains a difficult task because of variable tumour characteristics in terms of size, frequency, and appearance in various brain regions. When it comes to diagnosing and treating brain malignancies, the neuroimaging modality known as magnetic resonance imaging (MRI) is the one that is utilized the majority of the time, other neuroimaging modalities include computed tomography, positron emission tomography, and magnetic resonance imaging [7].

A brain tumour can be diagnosed and treated more effectively using an Magnetic resonance imaging scan. Accurate identification of brain abnormalities depends on the imaging equipment [8]. The living structure of the brain is examined with an MRI or computerized tomography (CT) scan. A CT scan studies the anatomy of the brain and provides comprehensive images of it. When compared to CT scanning, MRI is far more efficient and emits no radiation. By locating the damaged area, the MRI locates the abnormalities in the brain. The MRI was created to provide high-quality pictures and to provide greater information about the characteristics of various tissues. The abnormal cells that have formed from bodily tissues are what give the tumour its shape [9]. Only a portion of the MRI will provide the whole picture of the abnormal tissues because a tumour identifies different biologic tissues. The segmentation procedure is made more difficult by the variability in the brain's size, shape and strength. Using four slices, including An MRI scan using T1, T2, T1 contrast and FLAIR can detect a brain tumour [10].. The human check-up that uncovered the MRI brain tumour may have been flawed. The appropriate characteristics for classification have been extracted using an integration of many approaches. The Gabor filter examines if the picture has any certain frequency content in particular directions in a focused area [11]. Each component is taught by the Wavelet transform with a resolution appropriate to its current state [12].

A Network for Holistically Nested Edge Detection (NED) was employed as the neural network by R. Pourreza et al. [13] to increase segmentation accuracy while having a minimal processing cost. Computationally efficient preparation and post processing methods are used. This method's drawback is that it results in a fluctuating, uneven backdrop in the MRI picture. A technique called a Markov Random Field (MRF) with sparse representation that performs well and provides high accuracy in classification, was developed by Y. Li et al. [14]. This approach uses deep learning to evaluate tumours quantitatively. The Dynamic Classifier Selection Markov Random Field (DCSMRF) approach was created by A. Ahmadvand et al. [15] and has a more dependable and resilient initial segmentation that leads in smoother and more refined segmentation outcomes. SVM can be used for supervised classification to achieve higher accuracy, but it cannot be applied in this technique due to the lengthy processing times needed for the datasets used. Improved segmentation accuracy in far less period and a more stable method were created by G. Wang et al. [16] using an interactive segmentation structure based on deep learning. Adapting object-specific parameter modification should be part of the procedure. In the interactive method, the settings for each test picture need to be changed for better segmentation exactness.

J. Amin et al. [17] implemented an automated method that makes use of an SVM classifier of precisely and correctly assessing brain tumours and useful in improving categorisation. Erosion does not remove genuine tumour pixels, but it does remove superfluous pixels and lower the FPR.

This study focuses on the three techniques that have been created for segmenting and classifying brain tumours: After receiving the input sequence, the segmented module will separate the tumor into its constituent parts. The input is split up into sections using enhanced active contour model approach, and the feature is extracted using the discrete wavelet transform. Finally, a regularised extreme learning machine (RELM) for creating a precise classification method for brain tumours. The method begins by applying a min-max normalisation technique to pre- process the brain pictures in order to enhance the difference between the regions and its borders. In an experiment using the random holdout strategy, the performance of the classification accuracy enhanced from 93% to 96%, showing that the method outperformed present condition techniques.

The article is organised as follows: Introduction of the article is explained in Section-I, Proposed method is discussed in Section-II, the work's findings are presented in Section- III, and the study is bound up in Section- IV.

## II. Proposed Methodology

Our segmentation method's goal is to separate the brain tumour region from the MR images and provide the brain tumour’s status for diagnosis. Fig.1 depicts the methods which the authors have proposed in this paper.

*International Journal on Recent and Innovation Trends in Computing and Communication*
*ISSN: 2321-8169 Volume: 11 Issue: 3s*
*DOI: https://doi.org/10.17762/ijritcc.v11i3s.6155*
***Article Received**: 01 December 2022 **Revised**: 04 January 2023 **Accepted**: 12 January 2023*

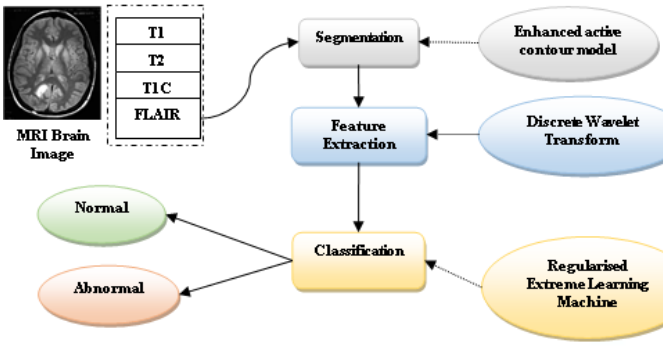


Fig 1. Block diagram of the proposed brain tumor segmentation system.

### (A) Image database

Cheng [18, 19] contributed the dataset that was used in this investigation. It includes 3064 MRI scans of brain tumours. There are three different planes: the frontal, lateral, and transverse plane was used to capture the photos of 233 individuals. 994 axial pictures, 1025 images of sagittal, and 1045 images of coronal were divided into three sets. The dataset includes three different forms of brain tumours: meningioma (1426 pictures) (1426 images) pituitary (708 pictures), and glioma (930 images). Each picture included a 512 × 512-pixel original size. The dataset's creator arranged the brain photos, assigned labels, and Patient ID, tumour boundary coordinates, and tumour mask images in data format for MATLAB. Several illustrations from the dataset include seen in Fig. 2.

### (B) Removing noise from the input image

For noise reduction in this step, we employed a modified bilateral filter. The steplike edge characteristics may be very effectively smoothed using a bilateral filter. The key issue, however, is that this filtering only performs effectively when the gradient changes are not particularly large. There are certain outliers in high-gradient changes, and the window cannot identify them. The trilateral filter, which features a slanted window to follow the high-gradient zones, is a modified version of this bilateral filtering. It functions in a similar manner to how bilateral filtering does. It discovers the gradient alterations, but with one distinction: it discovers the skewed gradient. The bilateral filter is extended by it. Trilateral filter can be used to clean up images that have been impacted by impulse noise. We applied this filter to both picture restoration and mixed noise de-noising. While maintaining the features of the image, this filter softens the edges of the picture. With the aid of a relatively small spatial window, it takes neighbouring pixel information into account and requires more iteration compared to bilateral filtering. It lowers the original picture's volatility and standard deviation.

### (C) Enhanced active contour model for Segmentation

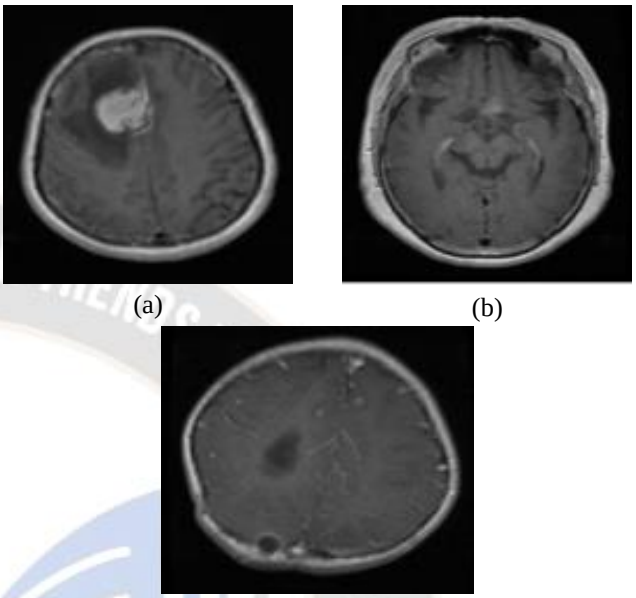

(a) (b)

(c)

Fig 2. Brain images examples taken from the dataset. (a) Meningioma brain tumour, (b) Pituitary brain tumour, (c) Glioma brain tumour

In this section, the enhanced active contour model for separating MRI images of brain tumors using both a local and a global intensity fitting prototype is explained. First, a global energy fitting prototype is used to get global image data so that the developing curve can be steered globally and the picture intensity both inside and outside the curve can be roughly calculated.
A local energy fitting prototype is then proposed to explain t he difference in intensity based -
on the specific difference in intensity and the adaptive pictur e difference. A hybrid region-based method that combines global and local weighting techniques is developed to improve the segmentation performance of brain tumor MRI images.

Typically, the contour function for segmenting MRI images is the Chan-Vese (C-V) model. The C-V model's ability to be far less sensitive to initialisation is one of its most appealing features. However, The C-V model fails to sequence model with non-uniform intensity because it ignores local image data. Then, medical pictures with intensity inhomogeneity are segmented using a local binary fitting (LBF) model. The LBF model works well with uniform intensity medical pictures and makes use of the kernel function. However, because of its localisation trait,

*International Journal on Recent and Innovation Trends in Computing and Communication*
*ISSN: 2321-8169 Volume: 11 Issue: 3s*
*DOI: https://doi.org/10.17762/ijritcc.v11i3s.6155*
***Article Received**: 01 December 2022 **Revised**: 04 January 2023 **Accepted**: 12 January 2023*

which might cause the model to get locked in local minima, this model is sensitive to the initialization of contours. This model is sensitive to the initialization of contours. To successfully implement both local and global intensity values in medical pictures, an enhanced active contour model based on local and global Gaussian intensity fitting model was developed. The input image was substituted with the segmented images, which was generated by the image of Gaussian convolution in the evolution equation. During the level set evolutionary process, the increasing quality of the differential image both within and outside the contour was modified to represent the average intensity of the actual picture. However, utilising the global Gaussian fitting energy alone is insufficient for a MRI image of brain tumors to be divided into segments for analysis. This study came up with a model that adds adaptive differential picture and local intensity fitting variance to the energy function to clarify the intensity and change of such targeted area. Our suggested model's energy function could be calculated as,

$$E_\varepsilon(f_1, f_2, C) = \alpha.\varepsilon^{giff} + \varepsilon^{liff} + \beta \int_v^{\cdot} \quad \delta_\varepsilon\big(\phi(x)\big) H_\varepsilon\big(\phi(x)\big) dx + \frac{\gamma}{2} \int_v^{\cdot} \quad (|\nabla\phi| - 1)^2 dx \tag{1}$$

$''\alpha''$ is the represented as fitting energy weight factor which varies between 0 and 1.

The third and fourth components in equation () are referred to as the length regularising term and the distance regularising term, respectively. In the LBF model, these two terms serve as the energy function. The global fitting energy term (or energy function) $\varepsilon^{giff}$ is created as,

$$\varepsilon^{giff}(\phi, C_1, C_2) = \omega_1 \int_v^{\cdot} \quad |I(x) - C_1|^2 H_\varepsilon\big(\phi(x)\big) dx + \omega_2 \int_v^{\cdot} \quad |I(x) - C_2|^2 \left(1 - H_\varepsilon\big(\phi(x)\big)\right) dx \tag{2}$$

The local fitting term ($\varepsilon^{liff}$) is constructed as,

$$\varepsilon^{liff}(\phi, f_1, f_2) = \rho \int_v^{\cdot} \quad \left|I` - I\right|^2 dx + (1 - 2\rho) \int_v^{\cdot} \quad v_1^2(x) H_\varepsilon\big(\phi(x)\big) dx + (1 - 2\rho) \int_v^{\cdot} \quad v_2^2(x) \left(1 - H_\varepsilon\big(\phi(x)\big)\right) dx \tag{3}$$

$\rho$ is the adaptive weighting function values between 0 and 0.5; $I`$ is the local adaptive picture and I is the actual picture. $v_1^2$, and $v_2^2$ are the local fitting functions. Which was used to roughly show how the local intensity changed both within and outside the contour in the sector of the Gaussian kernel. By maximizing a predetermined energy function, we may determine its value using the gradient descent flow equation. The adaptive weighting function significantly influences how the curve evolves, yet the contour is gradually converging on the basis of image similarity. By the time the forming curve reaches the object's edge, it will have been drawn in that direction by the local intensity variance data. The Fig. 3 shows the flowchart for the segmentation process using enhanced active contour model.

### (D) Discrete wavelets transform Feature Extraction

Using feature extraction, the valid or crucial information from the MRI scans is extracted. To extract the feature from the MRI, many methods were applied. The tumour image extraction is crucial to this segmentation procedure. In order to simplify the system and boost performance, the extraction in this tumour detection study uses the DWT-based brain tumour segmentation. It involves taking valuable information out of the segmented tumour picture (it may be size, shape, colour, and texture). The defined different characteristics are taken from MRI scans and shown in brain tumour pictures. Based on the MRI picture prototype, the tumour's segmented component has a distinct nature. It's taken and generated from these whole photos.

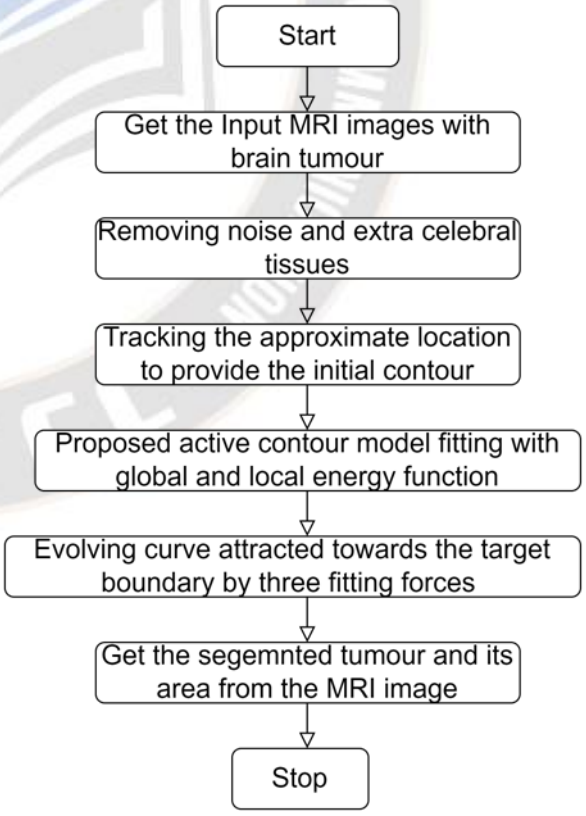


Fig. 3. Flowchart of segmentation process using active contour model

*International Journal on Recent and Innovation Trends in Computing and Communication*
*ISSN: 2321-8169 Volume: 11 Issue: 3s*
*DOI: https://doi.org/10.17762/ijritcc.v11i3s.6155*
*Article Received: 01 December 2022 Revised: 04 January 2023 Accepted: 12 January 2023*

The DWT was often used to investigate various level frequencies of distinct pictures using a range of scales. For extracting features from extraction, DWT is a more useful technique. The brain tumour MRI images are retrieved using discrete wavelet after the features from the coefficients are extracted. Importing wavelet-based localised frequency data, which is based on 2D DWT and other techniques, is crucial in this categorisation.

The multiscale approximation property of DWT makes it possible to examine photos with various amounts of resolution, making it a crucial tool for extracting features from tumour images. Multiscale analysis is used to properly extract MRI data.

It is possible to divide the 2D transform into four distinct sub-band resolutions, including combinations such as Low-Low (LL), Low-High (LH), High-Low (HL), and High-High (HH) (levels of frequencies in both forward and reverse orientations). There are essentially four distinct bands. framed depending on applying the DWT model to the Region of Interest.

The part of the image with high frequency, which are represented by LH2, HL2, HH2, LH3, HL3, and HH3 gives a detailed explanation of all directions including the parts of the MRI picturer that are completely flat, directional and diagonal, is dealt with in the second and third levels of decomposition shown in Fig. 4. We currently understand that LL1 stands for the approximate MRI original picture, which is processed for the subsequent level of decomposition. In order to get the appropriate level of picture resolution, this procedure is repeatedly repeated. The step is based on: First-order statistics: The two characteristics that are retrieved are the average and the variation from the mean. The simultaneous existence of two pixels. at particular relative locations is the subject of second order statistics.

(i) *Contrast:* It processes the local variation present in an image

$$\sum_{p,q} \quad (p-q)^2 M_{d,\theta}(p,q) \tag{4}$$

(ii) *Correlation:* It determines how a pixel is correlated to its neighbourhood pixel.

$$\sum_{p,q} \quad \frac{(p-\mu_x)(q-\mu_y)M_{d,\theta}(p,q)}{\sigma_x \sigma_y} \tag{5}$$

(iii) *Homogeneity:* It provides the similarity of pixel.

$$\sum_{p,q} \quad \frac{M_{d,\theta}(p,q)}{1+|p-q|^2} \tag{6}$$

(iv) *Entropy:* It assess of randomness of intensity image

$$\sum_{p,q} \quad M_{d,\theta} log_2\left[(M_{d,\theta}(p,q)\right] \tag{7}$$

(v) *Energy:* The sum of squared elements in the co-occurrence matrix (gray level) is returned.

$$\sum_{p,q} \quad (M_{d,\theta}(p,q)^2 \tag{8}$$


Fig 4. Input image with different levels of decomposition

### (E) Regularized Extreme learning machine

Due to its capacity to get around the drawbacks associated with the backpropagation approach, In most cases, we use the (RELM) regularized extreme learning machine, a classification and regression technique. The RELM is superior to other classifiers due to its quick training time and lack of complexity. To help radiologists and doctors identify the many types of brain tumours, we suggest an algorithmic system for classifying brain tumours. Due to its regularisation property, which minimises the overfitting issue, and its speed during training, we choose a RELM classifier. RELM describes a type of feedforward neural network (FNN) that has input and exit layers. The input layer's biases are randomly chosen to determine the output layer's weights. The data from the brain characteristics discovered during the previous stage are used to train the RELM classification model. The type of brain tumor is then accurately classified using the trained RELM model. This step's input and output are shown in Figure. 5.

The proposed solution has a few parameters that need to be established. The values of these parameters are chosen for the tests using the grid search approach and the expertise in machine learning and image intelligence. As was already indicated, several of the approach's parameters were selected

*International Journal on Recent and Innovation Trends in Computing and Communication*
*ISSN: 2321-8169 Volume: 11 Issue: 3s*
*DOI: https://doi.org/10.17762/ijritcc.v11i3s.6155*
*Article Received: 01 December 2022 Revised: 04 January 2023 Accepted: 12 January 2023*

empirically. The number of eigenvectors that creates the best representative feature and the quantity of highly accurate hidden nodes in RELM, for instance, were both tested in the tests by the authors using various numbers of eigen vectors and RELM's hidden nodes.

Algorithm: Brain Tumour Categorisation

**Input :** Training data and testing data, and parameters of features that were taken of brain.
Training brands

**Output :** ($V_q$) Testing brands

**Begin**

**Training Stage**

Initialization of Weights and Biases

Randomly selecting the weights ($w_p$) and biases ($b_q$) from the inputs ($a_i$) for the input layer of RELM

Computation of Matrix

Hidden layer matrix (H) calculation

$$H = \begin{bmatrix} g(w_1 a_1 + b_1) & \cdots & g(w_M a_1 + b_M) \\ \vdots & \ddots & \vdots \\ g(w_1 a_N + b_1) & \cdots & g(w_M a_N + b_M) \end{bmatrix}$$

Weight and target matrices ($\beta$ and T) calculation

$$\beta = \begin{bmatrix} \beta_1^T \\ \cdot \\ \cdot \\ \beta_M^T \end{bmatrix}, \text{ and } T = \begin{bmatrix} t_1^T \\ \cdot \\ \cdot \\ t_{NM}^T \end{bmatrix},$$

**Testing Stage**

Computation of Matrix

Hidden layer matrix (H) calculation

Output weights computation

$$\dot{\beta} = (H^T H + \lambda I)^{-1} H^T T$$

Output matrix ($O_j$) Computation

$$O_j = \dot{H}\dot{\beta}$$

Location of testing class brands ($l_j$) l, where j$\epsilon$ $L$, and L is the numbe of classes

$$l_j = \underbrace{\arg}_{j \epsilon L} \max(O_j)$$

Return Testing brands ($l_j$)

Fig 5. Brain Tumour classification using RELM

*International Journal on Recent and Innovation Trends in Computing and Communication*
*ISSN: 2321-8169 Volume: 11 Issue: 3s*
*DOI: https://doi.org/10.17762/ijritcc.v11i3s.6155*
***Article Received**: 01 December 2022 **Revised**: 04 January 2023 **Accepted**: 12 January 2023*

## III. Experimental Results

Cheng contributed the dataset that was used in this research, as was discussed in section II. In this study, some of the parameters for the suggested methods need to be initialized. Particularly, certain of the approach's parameters were selected empirically. For instance, we performed trials with various eigenvector and hidden node counts before choosing the eigenvector count that yields the best representative feature and precision in terms of the fraction of RELM's hidden nodes. Between 150 and 350 eigenvectors are picked, and 2250 is chosen as the hidden value for the RELM.

On the basis of holdout and 5-fold cross validation approaches, several experiments are run. We separated the dataset into two sets for the holdout technique: a training set that comprises 70% of the dataset and remaining 30% for the testing data. As opposed to that, dataset is split into five sets for the 5-folds cross validation. Whereby the four sets are used for training and one set is chosen for testing. There are five iterations of this process. During the testing phase, to evaluate different types of brain tumors, we compute their confusion matrices.

The confusion matrices for classifying brain tumours are displayed in Figure 6 utilising various Eigenvectors (EVs) from PCA for the holdout method. The accuracy results from these matrices are determined as follows:

$$Accuracy = \frac{(TPR+TNR)}{(TPR+FPR+TNR+FNR)} \quad (9)$$

where FNR and TNR stand for false and true negative rates and FPR and TPR stand for false and true positive rates, respectively.

| | Meningioma | Pituitary | Glioma |
|---|---|---|---|
| Meningioma | 258 | 17 | 28 |
| Pituitary | 44 | 348 | 6 |
| Glioma | 8 | 3 | 552 |
| Accuracy | | 94.63 % | |

(a) EACM - IDWT with RELM Confusion matrix (EVS = 150)

| | Meningioma | Pituitary | Glioma |
|---|---|---|---|
| Meningioma | 269 | 13 | 21 |
| Pituitary | 39 | 356 | 3 |
| Glioma | 5 | 2 | 556 |
| Accuracy | | 94.93% | |

(b) EACM - IDWT with RELM Confusion matrix (EVS = 250)

| | Meningioma | Pituitary | Glioma |
|---|---|---|---|
| Meningioma | 264 | 15 | 24 |
| Pituitary | 41 | 353 | 4 |
| Glioma | 6 | 3 | 554 |
| Accuracy | | 96.22 % | |

(c) EACM - IDWT with RELM Confusion matrix (EVS = 350)

Fig. 6. Results of confusion Matrices

We can see from Figure 6 that 350 is the optimum EV value. As a result, this number will be fixed and chosen to reflect the important elements that may be derived from brain scans.

Figure 7 shows how EACM - IDWT with RELM classifier performs in comparison to other relevant techniques. Additionally, we observed that the classification accuracy using improved discrete wavelets transform (IDWT) descriptor is higher than the classification accuracy using conventional discrete wavelets transform (CDWT).

Table 1 evaluates the suggested technique by comparing the accuracy of classification of our suggested methodology to that of using the most recent methods. We can observe that the

Classification accuracy attained using our suggested method is superior to that attained utilising the most recent methodologies (e.g., convolutional neural network, random

*International Journal on Recent and Innovation Trends in Computing and Communication*
*ISSN: 2321-8169 Volume: 11 Issue: 3s*
*DOI: https://doi.org/10.17762/ijritcc.v11i3s.6155*
***Article Received**: 01 December 2022 **Revised**: 04 January 2023 **Accepted**: 12 January 2023*

forest, and radial basis function, etc). The ability to extract the significant characteristics in reducing the kind of brain tumours utilising the feature extraction approach and the RELM classification method is what has led to this improvement in classification accuracy.

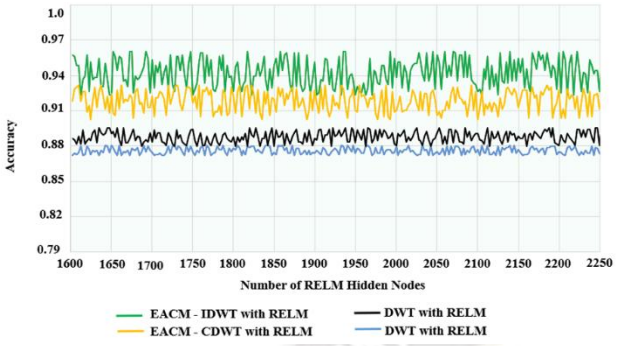


Fig. 7. Results of brain T images taken from the dataset.

Table. 1. Accuracy of brain tumour classification: a comparative of proposed approaches with those described in the literature

Table. 1. Accuracy of brain tumour classification: a comparative of proposed approaches with those described in the literature

| Reference | Approach | Image Size | Accuracy |
|---|---|---|---|
| [21] | Convolutional neural network | 256 x 256 | 91.43 % |
| [21] | Random Forest | 256 x 256 | 90 % |
| [22] | Support Vector Machine - Radial Basis Function | 256 x 256 | 91.51 % |
| Proposed Method | EACM – IDWT - RELM | 256 x 256 | 96.25 % |

## IV. Conclusion

This study proposed a three-step method for effectively classifying brain tumours. First, an enhanced active contour model is intensively processing the required values from brain pictures. The most crucial characteristics are then retrieved using improved DWT, an effective technique. Finally, the RELM classifier is used to categorise brain cancers. A new publicly available dataset of pictures of brain tumours is used to assess and compare the suggested approach's classification accuracy. This dataset includes 3064 brain scans from 233 people that show three different forms of brain tumours. In the trials, 5-folds cross validation and holdout (70% training and 30% testing) are used.. According to the experimental findings, the EACM – IDWT - RELM feature extraction approach is more accurate than other conventional methods. Additionally, the findings proved that the suggested technique did a better job of classifying brain tumors than the most recent techniques. We want to use the proposed method to resolve another biological classification issue and conduct a comparison analysis of several machine learning classifiers.

## References

[1]. Global Cancer Observatory. https://gco.iarc.fr/. Accessed 08 Nov 2021.
[2]. Cancer statistics, 2020—Siegel—2020. CA Cancer J Clin. Wiley Online Library. https://doi.org/10.3322/caac.21590.
[3]. Differentiating tumor recurrence from treatment necrosis: a review of neuro-oncologic imaging strategies |Neuro-Oncology Oxford Academic. https://academic.oup.com/neuro-oncology/article/15/5/515/1012031. Accessed 08 Nov 2021.
[4]. Field M, Witham TF, Flickinger JC, Kondziolka D, Lunsford LD. Comprehensive assessment of hemorrhage risks and outcomes after stereotactic brain biopsy. J Neurosurg. 2001;94(4):545–51. https://doi.org/10.3171/jns.2001.94.4.0545.
[5]. Zhou M, et al. Radiomics in brain tumor: image assessment, quantitative feature descriptors, and machine-learning approaches. Am J Neuroradiol. 2018;39(2):208–16. https://doi.org/10.3174/ajnr.A5391.
[6]. Clinical evaluation of a fully-automatic segmentation method for longitudinal brain tumor volumetry Scientific Reports. https://www.nature.com/ articles/srep23376/. Accessed 08 Nov 2021.
[7]. Wesseling P, van den Bent M, Perry A. Oligodendroglioma: pathology, molecular mechanisms and markers. Acta Neuropathol. 2015;129(6):809. https://doi.org/10.1007/s00401-015-1424-1.
[8]. S. Bauer, R. Wiest, L. P. Nolte, and M. Reyes, “A Survey of MRI-Based Medical Image Analysis for Brain Tumor Studies,” Phys. Med. Biol., vol. 58, no. 13, pp. R97–R129, 2013.
[9]. T. D. Pham, “Image Segmentation using Probabilistic Fuzzy C-Means Clustering,” Proc. IEEE Int. Conf Image Process., pp. 722–725, 2001.
[10]. P. Anbeek, K. Vincken, and M. Viergever, “Automated MS-Lesion Segmentation by K-Nearest Neighbor Classification,” MIDAS J. - MS Lesion Segmentation (MICCAI 2008 Work., pp. 1–8, 2008.
[11]. C. Liu and H. Wechsler, “Gabor Feature-based Classification using the Enhanced Fisher Linear Discriminant Model for Face Recognition,” IEEE Trans. Image Process., vol. 11, no. 4, pp. 467–476, 2002.
[12]. M. Kociolek, A. Materka, M. Strzelecki, and P. Szczypinski, “Discrete Wavelet Transform – Derived

*International Journal on Recent and Innovation Trends in Computing and Communication*
*ISSN: 2321-8169 Volume: 11 Issue: 3s*
*DOI: https://doi.org/10.17762/ijritcc.v11i3s.6155*
*Article Received: 01 December 2022 Revised: 04 January 2023 Accepted: 12 January 2023*

Features for Digital Image Texture Analysis," Int. Conf. Signals Electron. Syst., pp. 163–168, 2001.

[13]. R. Pourreza, Y. Zhuge, H. Ning, and R. Miller, "Brain Tumor Segmentation in MRI Scan Using Deeply-Supervised Neural Networks," brainless, Lect. Notes Comput. Sci., vol. 10670, pp. 320–331, 2018.

[14]. Y. Li, F. Jia, and J. Qin, "Brain Tumor Segmentation from Multimodal Magnetic Resonance Images via Sparse Representation," Artif. Intell. Med., vol. 73, pp. 1–13, 2016.

[15]. A. Ahmadvand, M. R. Daliri, and S. M. Zahiri, "Segmentation of Brain MR Images using a Proper Combination of DCS based method with MRF," Multimedia. Tools Appl., vol. 77, no. 7, pp. 8001–8018, 2018.

[16]. G. Wang et al., "Interactive Medical Image Segmentation Using Deep Learning with Image-Specific Fine Tuning," IEEE Trans. Med. Imaging, vol. 37, no. 7, pp. 1562–1573, 2018.

[17]. J. Amin, M. Sharif, M. Yasmin, and S. L. Fernandes, "A Distinctive Approach in Brain Tumor Detection and Classification using MRI," Pattern Recognit. Lett., pp. 1–10, 2017.

[18]. J. Cheng, ''Brain tumor dataset (version 5),'' 2017. doi: 10.6084/m9.figshare.1512427.v5.

[19]. J. Cheng et al., ''Enhanced performance of brain tumor classification via tumor region augmentation and partition,'' PLoS One, vol. 10, no. 12, 2015, Art. no. e0144479.

[20]. S. M. K. Hasan and M. Ahmad, "Two-Step Verification of Brain Tumor Segmentation using Watershed-Matching Algorithm," Brain Informatics, vol. 5, 2018.

[21]. J. Paul, ''Deep learning for brain tumor classification,'' M.S. thesis, Dept. Comput. Sci., Vanderbilt Univ., Nashville, TN, USA, May 2016.

[22]. N. Abiwinanda, M. Hanif, S. T. Hesaputra, A. Handayani, and T. R. Mengko, ''Brain tumor classification using convolutional neural network,'' in World Congress on Medical Physics and Biomedical Engineering. Singapore: Springer, 2018, pp. 183–189.